Robotica: page 1 of 8. © Cambridge University Press 2011
doi:10.1017/S0263574711000014

Experimental verification of soft-robot gaits evolved using a lumped dynamic model

Frank Saunders†,*, Ethan Golden‡, Robert D. White† and Jason Rife†

†*Department of the Mechanical Engineering, Tufts University, Medford, MA, USA*
‡*Department of the Biology, Tufts University, Medford, MA, USA*

(Received in Final Form: January 5, 2011)

SUMMARY
When generating gaits for soft robots (those with no explicit joints), it is not evident that undulating control schemes are the most efficient. In considering alternative control schemes, however, the computational costs of evaluating continuum mechanic models of soft robots represent a significant bottleneck. We consider the use of lumped dynamic models for soft robotic systems. Such models have not been employed previously to design gaits for soft robotic systems, though they are widely used to simulate robots with compliant joints. A major question is whether these methods are accurate enough to be representations of soft robots to enable gait design and optimization. This paper addresses the potential "reality gap" between simulation and experiment for the particular case of a soft caterpillar-like robot. Experiments with a prototype soft crawler demonstrate that the lumped dynamic model can capture essential soft-robot mechanics well enough to enable gait optimization. Significantly, experiments verified that a prototype robot achieved high performance for control patterns optimized in simulation and dramatically reduced performance for gait parameters perturbed from their optimized values.

KEYWORDS: Soft robot; Biomimetic design; Gait optimization.

1. Introduction

The construction of robots from highly deformable materials, such as elastomers, will enable enhanced mobility in confined spaces. We will use the term *soft robot* to describe this class of device, which uses soft materials to attain flexibility in the absence of explicit joints. The ability of soft robots to flex and squeeze through orifices smaller than their frontal area makes them attractive for applications in surgery, disaster recovery, and covert access.

Implementing an efficient locomotion strategy is a significant challenge in designing soft robots (such as the caterpillar-like robot depicted in Fig. 1). In the absence of a conventional rigid "skeleton," actuators introduce large deformations when transmitting forces through the robot structure. Owing to these deformations, it is difficult to design effective controllers.

*Corresponding author. E-mail: frank.saunders@tufts.edu

We propose that the lumped-parameter dynamic model is an effective tool for the design and optimization of gaits for soft and biologically inspired robots. The lumped-parameter systems consist of a set of interconnected elements with parameters (mass, inertia, stiffness, and damping) that represent larger segments of the soft-robot structure. Since the lumped dynamic model abstracts the continuum model, it is not immediately evident that the lumped approach can resolve system dynamics well enough to enable control design.

The primary focus of this paper is to use experiments to evaluate the effectiveness of the lumped dynamic model in enabling gait design for a soft, caterpillar-inspired robot. The remainder of the paper is organized as follows. The second section provides a brief overview of caterpillar crawling and control design for caterpillar-like robots. The third section will describe the prototype hardware used for our experiments and the fourth section will describe the lumped dynamic model used to simulate the prototype hardware. The fifth section will describe a set of gait patterns evolved by incorporating the lumped dynamic model into a genetic algorithm and the sixth section will compare the simulated gaits to the experimentally acquired data (using a VICON motion capture system). The final section will summarize the results and conclude the paper.

2. Background

In order to guide the development of gaits for a soft caterpillar-like robot, it is instructive first to consider insights gained from related classes of bio-inspired robots, such as snake-like robots, as well as from actual, biological caterpillars. Previous efforts to develop undulating rigid-body robots provide a limited context for designing soft-robot gaits. Fundamentally, soft-body robots introduce almost infinite degrees of freedom, and in particular, degrees of freedom involving compression and extension, which are not generally present in rigid-body, bio-inspired robots (demonstrated in Fig. 2). That rigid-body robots tend to exhibit significant flexibility in bending, but not in tension and compression, may explain why longitudinal wave patterns are so often used to generate locomotion for snake-like robots.[1–3] Other undulating, bio-inspired robots, such as salamanders, have also been controlled by wave-like gaits, such as regular patterns involving out-of-phase oscillation between bilateral actuators.[4,5]

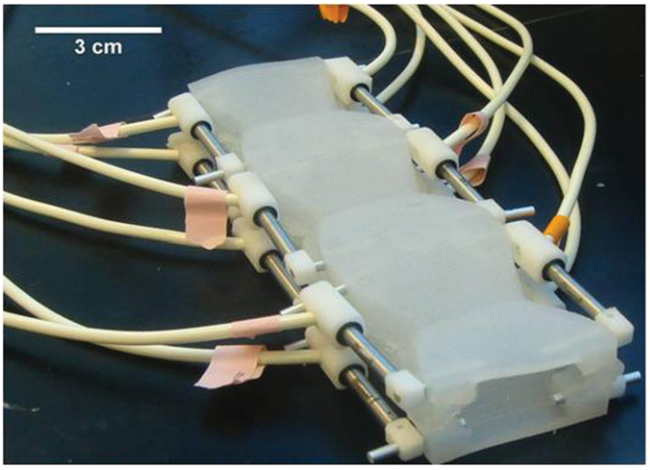

Fig. 1. Caterpillar-inspired biomimetic robot.

Fig. 2. Elastically deformed robot body.

The motions of natural caterpillars also consist of "waves" that proceed from the posterior to the anterior of the animal.[6] In the caterpillar control system, however, muscle actuation patterns are not necessarily simple undulations (e.g., patterns of opposing positive and negative torques that propagate as a self-similar traveling wave). Evidence suggests that caterpillar muscles fire in a sequence that progresses in a phased (but not repeated) manner through each of the caterpillar's body segments.[7] Patterns of muscle inactivation are also nonrepeating. This is significant since muscles may contribute to body motion (by introducing damping forces or by maintaining body turgor) even when they are not activated.[8] The fact that control patterns for a soft-bodied animal are not self-similar traveling waves (undulations) suggests that effective gaits for an artificial caterpillar-like soft robot may likewise be non-undulating.

Observations of caterpillars also suggest that a surprisingly simple neuromuscular system may be sufficient to control a vast number of degrees of freedom.[7] The caterpillar is capable of many types of motions, such as reaching, probing, rolling, and strike reflex movements.[6] All of these motions are generated by a neuromuscular control system in which each muscle is typically actuated by only one motorneuron.[8] That this simple, distributed control system can generate such a wide variety of motions suggests that some control functions are imbedded in the animal's material composition and body mechanics, a principle that sometime is called *embodiment*.[9] Applying this lesson to soft-robot applications, it may be possible to use a simple control system to generate a range of movement behaviors, if the design of the physical structure and the controls are tightly coordinated.

In this context, the primary goal of our work is to develop effective gaits to generate locomotion in a soft robot, by which we mean a robot with a large number of degrees of freedom and no explicit rigid or compliant joints. Based on our biological model, we seek a relatively low-complexity controller, which is not necessarily a purely undulating control sequence, represented as a self-similar traveling wave of control commands.

Some work has been done previously to control soft robots, but this work has not focused specifically on gait design. In fact, most of the prior work on soft robots has focused on novel actuation strategies, generally involving gross deformations of the robot rather than coordinated activation of distributed actuators.[10,11] For example, the proposed soft-robot locomotion strategies include the use of gel-like actuators comprising electro-active polymers that enable simultaneous deformation of the entire robot volume, the use of toroidal flexure devices that operate in the manner of a radially symmetric treadmill, and the use of peristalsis in the manner of leeches and worms.[2,12,13]

Given the lack of a clear methodology for developing gaits for soft robots, we ask a fundamental question. *Can the existing tools for rigid-body simulation be adapted for use in designing gaits for soft robots?* With this question in mind, we consider the approach of evolving soft-robot gaits using lumped dynamic models. Such models can be simulated using commercially available multibody dynamics software. Lumped dynamic models have been proposed previously for a range of biological systems, primarily animals with rigid skeletons[14] or exoskeletons[15] and compliant joints. Lumped dynamic models have also been used to simulate bio-inspired robots with rigid frames and joint or contact compliance.[16–19] Lumped models have not been applied previously to develop gaits for truly soft robots. Rather, in an effort to obtain as much accuracy as possible, prior efforts to simulate and model soft biological and bio-inspired systems, such as real octopus arms and octopus-inspired robot arms, have focused on more complex continuum (finite difference) models rather than simpler lumped-element models.[20–22]

Though continuum models may be required to fully resolve the dynamics of a soft system, we hypothesize that continuum modeling techniques (such as a finite-element analysis (FEA)) may not always be necessary for the optimization of soft-robot gaits. In order to test this hypothesis, we constructed a caterpillar-like soft robot. Using this robot, we developed a corresponding lumped-parameter model, optimized gaits for that model using a genetic algorithm, and implemented those gaits on the physical hardware to evaluate their effectiveness.

3. Hardware

In order to provide a test bed for designing soft-robot control schemes, a prototype caterpillar-like robot was constructed. The robotic system consists of a highly deformable elastomer body shell actuated by pneumatic pistons (see Figs 1 and 3). Actuation of the soft-robot body was achieved by an external air supply that powered the robot's 12 pneumatic pistons under the control of 12 independent off-board solenoid valves. For the purpose of this paper, each left–right pair

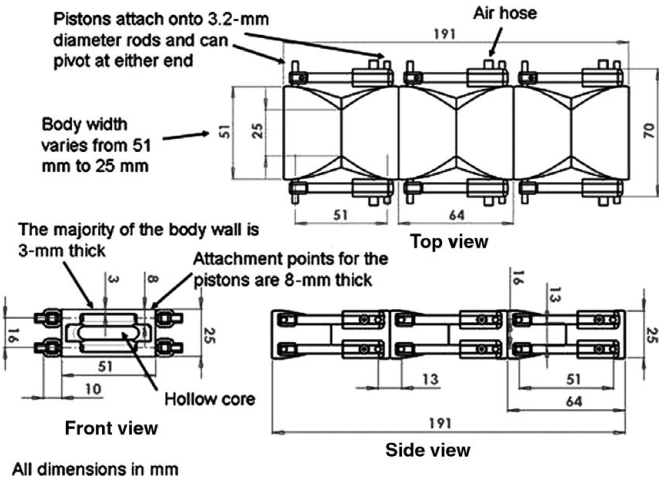

Fig. 3. Mechanical drawing of the bio-inspired caterpillar robot.

of solenoid valves is fired in parallel, so that only six independent control actions are present, and the robot body moves predominantly in a two-dimensional (2D) fashion in the *x*–*y* plane.

The body of the pneumatic crawling device was constructed from two symmetrical pieces of cast silicone elastomer (Dragonskin brand addition-cure rubber, Smooth-On Inc., Easton, PA). Half-bodies were cast in a two-part mold constructed from ABS plastic in a 3D printer (Dimension sst1200, Stratasys, Inc., Eden Prairie, MN). Prior to molding, 24 aluminum rods of 3.2-mm diameter were inserted through holes in the mold to create attachment points for the externally mounted pneumatic piston. The ABS mold was filled using a vacuum-casting machine (MCP-10, MCP Corporation, Manchester, UK). Symmetrical half-bodies were then adhered to each other with Dragonskin to create a complete robot body shell.

After the silicone body shells were cured, demolded, and bonded together, the 12 pneumatic actuators were attached. The linear pneumatic actuators (Clippard Instrument Laboratory, Cincinnati, OH), including the mounting hardware, are 51-mm long in their resting state and extend to 62 mm in length when supplied with pressurized air. The air supply was controlled via normally closed solenoid valves that are driven either fully open or fully closed by a computer with H-bridge motor drivers controlled by National Instruments Labview software (National Instruments, Austin, TX). By altering sequence, timing, and duration of airflow, a series of deformations could be produced in the elastomeric body of a crawler.

4. Lumped Dynamic Model

This section describes the procedure used to generate a lumped dynamic model for our soft-robot hardware. For the present study, a 3D rigid-body dynamics simulation with iterative contact resolution, the PhysX solver (Nvidia, Santa Clara, CA), was used to simulate the model.

In order to accelerate computation, we modeled the continuum structure of the experimental system (with its infinite number of degrees of freedom) using a lower order lumped dynamic model. In short, our approach was to identify repeated segments along the robot body and to split each segment into a pair of lumped masses. This split allows for a degree of bending and compression within each body segment (as well as between body segments). For our caterpillar-like soft robot, the resulting model consists of six lumped masses. Figure 4 compares this lumped approximation to the original 3D CAD drawing of the prototype robot. Model segments were not assigned a shape, except for the purposes of collision detection with the ground; segments were represented as rectangular prisms for this purpose.

The lumped stiffness parameters were estimated by applying finite element processing (5-node tetrahedral in Cosmos) to a 3D CAD model (developed in Solidworks). Specifically, bending and axial compression were modeled using rotational and torsional springs placed at the prismatic-spherical joints between each of the six subsegments illustrated in Fig. 4. Two FEAs were considered, one spanning adjacent body segments (S1–S2, S3–S4, S5–S6) and the second for an individual body segment (S2–S3, S4–S5). These FEA models are illustrated in Fig. 5. The FEA material properties were assigned to match those of the elastomer material used to fabricate the robot body ($\rho = 950\,\mathrm{kg/m^3}$, E = 435 KPa, $\upsilon = 0.33$). For each test section, two analyses were performed: an axial test to determine linear stiffness and a rotational test to determine torsional stiffness. For both axial and rotational analyses, one end of the test section was rigidly constrained. At the free end of the test section, a normal force of 0.1 N was applied for axial analysis, and a transverse force of 0.01 N was applied for rotational analysis. Based on the observed displacements during axial loading, linear spring constants were computed as 1040 N/m at a flexure and 446 N/m within a segment. For the torsional analysis, the transverse load resulted in a deformation of the test section's centerline from rest. Based on the change in the centerline angle at the free end, a rotational spring constant was computed as 0.12 Nm/rad at the flexures and 0.07 Nm/rad within a body segment. The lumped damping parameters, both axial and rotational, were defined at each joint assuming a linear model. Since the body does not oscillate when perturbed, values were set assuming critical damping. The lumped mass and inertia parameters were determined using a volume fill of the 3D CAD model.

The external forces acting on the soft robot in simulation included gravity, friction, and actuator forces. Gravity was defined to act perpendicular to the ground plane. Friction was

Fig. 4. Segmentation of structure.

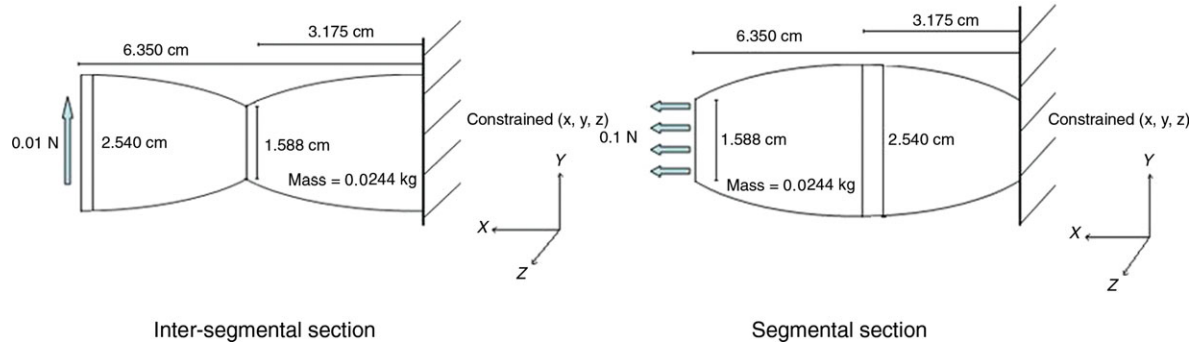

Fig. 5. Linear FEA for segmental and rotational FEA for intersegmental sections.

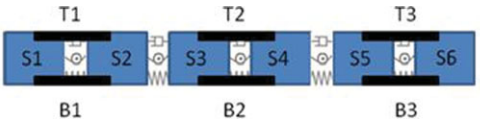

Fig. 6. Actuator pair locations.

modeled as infinite to enforce a nonslip condition between the robot and the ground. This condition was representative, since the robot's polymer body had a high friction coefficient when mated with the ground. For the pneumatic actuators, a periodic control signal for actuation was assumed. Control commands were allowed to turn the pneumatic actuators on and off at particular times during the gait period. Actuator attachment points were defined for each pneumatic cylinder, and the actuator forces were simulated to act along the line between these points. A restorative spring ($k = 63$ N/m) was also applied between the actuator attachment points to mimic return springs in the pneumatic piston hardware. The minimum and maximum distances between actuator attachment points were constrained to represent the maximum and minimum lengths of the physical actuators. When an actuator was on, it would produce a constant force (8.8 N) and extend until it hit the maximum displacement length. Upon the actuator turning off, the restorative spring would take the actuator back to its initial minimum length.

5. Evolved Gaits

Using a genetic algorithm, we simulated and evolved control patterns to maximize gait performance. Gait patterns were assumed to be periodic. Performance (or *fitness*) was defined as the distance the model traveled over one gait cycle.

For both the simulated and real robots, movement is the result of activating and deactivating the robot's 12 pneumatic actuators. In order to constrain model movements to a straight path, actuator commands were issued with lateral symmetry. Hence, open-loop control commands were only required for six actuator pairs (see Fig. 6). The gait period (T), over which actuator commands were repeated, was an evolved parameter. For each actuator pair (j), the activation time (a_j) and deactivation time (d_j) were specified as fractions of the gait period. Each control pattern was thus defined by a vector of 13 parameters, called the *genotype* ($\boldsymbol{G}$):

$$\boldsymbol{G} = [a_{T1}\ a_{T2}\ a_{T3}\ a_{B1}\ a_{B2}\ a_{B3}\ d_{T1}\ d_{T2}\ d_{T3}\ d_{B1}\ d_{B2}\ d_{B3}\ T].$$

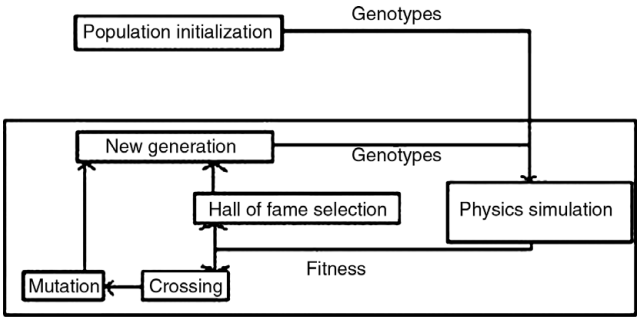

Fig. 7. Genetic algorithm diagram.

The genetic algorithm evolved a population of genotypes, iteratively tuning parameter values by favoring control patterns that resulted in high performance. Although details of the genetic algorithm methodology have been presented previously,[23] a brief overview is given here. A flow diagram for the genetic algorithm is illustrated in Fig. 7. The algorithm was initialized by randomly selecting genotype parameters for each member of the population. Each of these genotypes was subsequently evaluated using a dynamic simulation, which assessed distance traveled in a period of simulated time. The top 10 performing models were then placed into a hall of fame. These genotypes were preserved for the next generation without modification. The remainder of the next generation was then created with a "roulette wheel" method of combining (or *crossing*) genotypes from the current generation. This approach favors the selection of the most-fit genotypes by assigning every individual in the current population a selection probability (a portion of a roulette wheel) proportional to its fitness. Using this approach, pairs of genotypes from the current generation (or *parents*) were selected and crossed to create two new genotypes (or *children*). The crossing operation exchanges the first N parameters of the genotype vectors from each of the parents to create new genotypes for each child. The value of N was generated randomly for each new generation. Random mutations of genotype parameters also occurred. For any genotype parameter, the probability of mutation was 10%; the value for a mutated parameter was chosen randomly, by the same procedure used for parameter initialization.

Population size remained fixed between generations. In this work, the genetic algorithm was run for 150 generations with a population size of 200 members. After 150 generations, the top performers included a variety of

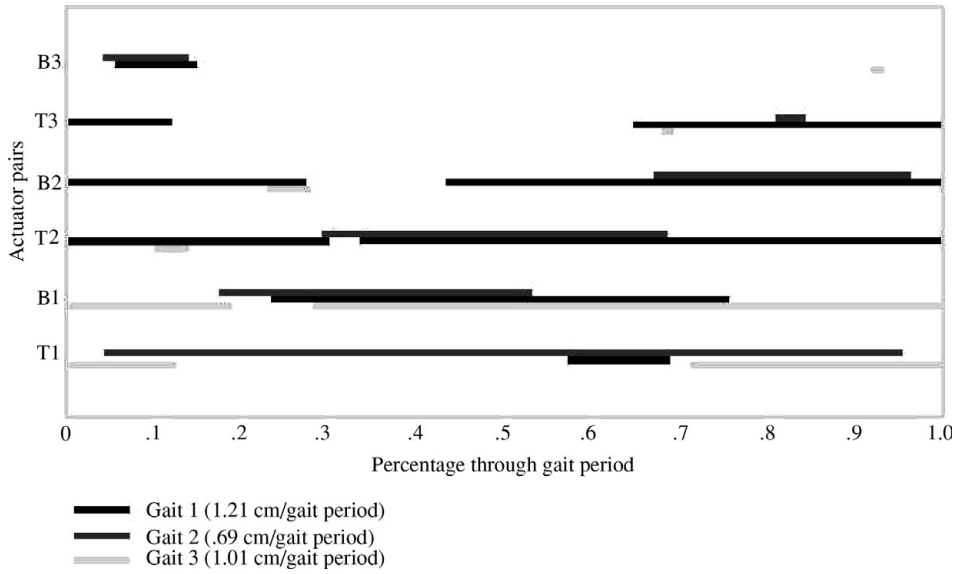

Fig. 8. Evolved gait patterns.

different gait periods with similar fitness values but widely varying control patterns.

For the purposes of experimentally validating the simulation, 10 of the best genotypes in the final generation were implemented using our hardware prototype. In order to promote diversity in this set of 10 genotypes, half were selected from within the hall of fame and half from outside. As representative examples, three of these gaits are illustrated in Fig. 8 (where solid lines represent activation of an actuator). The labels for each actuator (T1–T3 on top, and B1–B3 on bottom) are consistent with the labels defined in Fig. 6. As can be seen in Fig. 8, the individual actuator commands do not conform to traveling-wave patterns.

6. Experimental Evaluation

The evaluation of gait designs was performed experimentally using the soft-robot prototype. Three quantitative studies were performed to assess the suitability of the lumped dynamic model to support the control design. The first study, which considered all 10 gaits, compared travel distances achieved by the prototype hardware to those predicted by simulation. A second study compared motion-capture measurements to the simulated gait kinematics for a trio of gaits (those shown in Fig. 8). The final quantitative study considered the effect of perturbations of gait duration on travel speed for these three gaits.

For the first quantitative study, which compared predicted to actual travel distances,[24] tests were repeated five times for each of the 10 gaits. The results are summarized in Fig. 9. This figure compares the actual distance traveled to the predicted one. Error bars indicate one standard deviation variations in the ratio of the actual to the predicted distance traveled. On the right side of Fig. 9 is a box plot of the ratio between actual and predicted distances traveled for all the gaits. The range of actual distance traveled was between 11% and 74% of the simulated distance, considering all outliers. The mean distance ratio for all 50 tests was 35%. Mean values for individual gaits were close to this 35% level, demonstrating consistency in the error of the simulated travel distance.

The second quantitative study used the motion capture data to enable a more resolved comparison of the kinematics for the actual and simulated robots. For this experiment, only three gait patterns were considered (those from Fig. 8). A VICON© system was used to track six markers on the hardware. The markers were attached to the top of the robot prototype, as illustrated in Fig. 10. Matching locations were also tracked in the simulation to enable a motion comparison.[25]

The kinematics experiments showed a close correlation between the timing of specific movements for the experimental and simulated robots. Results for a representative gait pattern are illustrated in Figs 11 and 12. Similar results were obtained for all three gait patterns tested. Figure 11 plots vertical (y) displacement, and Fig. 12 plots horizontal (x) displacement as a function of time. The transverse (z) displacement was essentially zero for these experiments, and is not plotted. In the figures, the simulated motion is solid black, while the hardware's motion is a dashed line. The figures illustrate approximately two-and-a-half gait cycles.

The final qualitative analysis evaluated the impact of gait period on robot speed for each of the evolved actuation patterns. These tests were performed to assess how closely the evolved actuation patterns were matched to the specific morphology of the hardware prototype. For these tests, only the overall duration of the gait period was altered. Actuators were always activated or deactivated at the same percentage gait period (as illustrated in Fig. 8). In these tests, it was observed that the distance traveled by the robot hardware was adversely affected as the gait period deviated from the optimal evolved location. Figure 13 shows distances achieved per gait cycle as a function of gait duration. It is clear that the evolved gait period is optimal for each case tested.

In order to provide a baseline to interpret the performance of the evolved gaits, an undulating gait was also studied. The activation pattern for this gait was a traveling wave, as

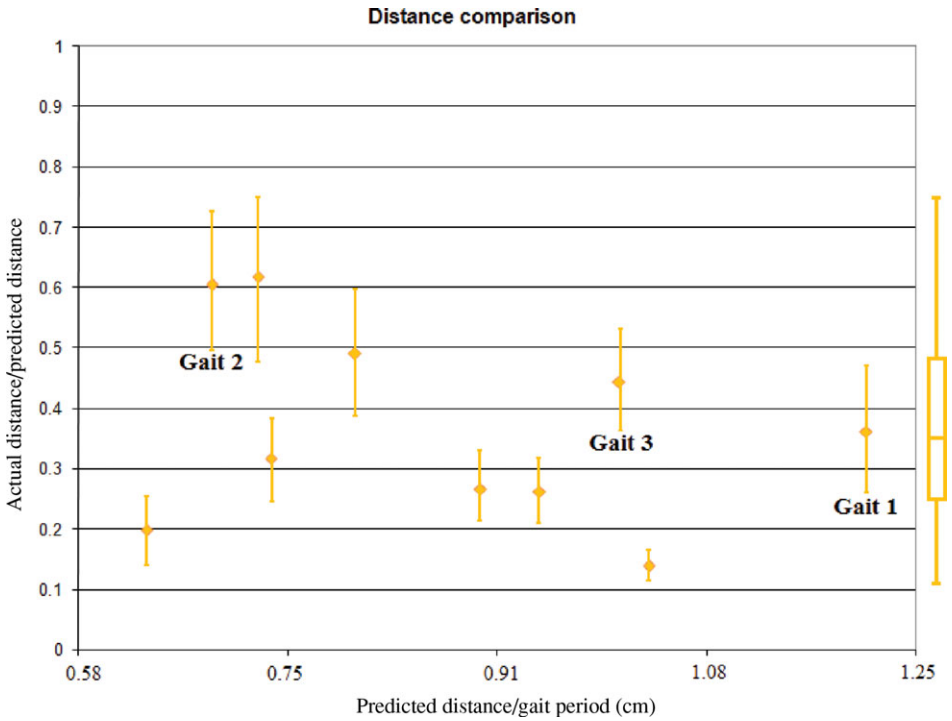

Fig. 9. Simulation to experiment comparison.

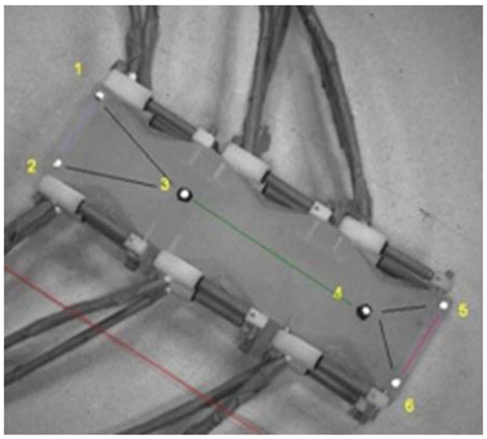

Fig. 10. Point tracking locations.

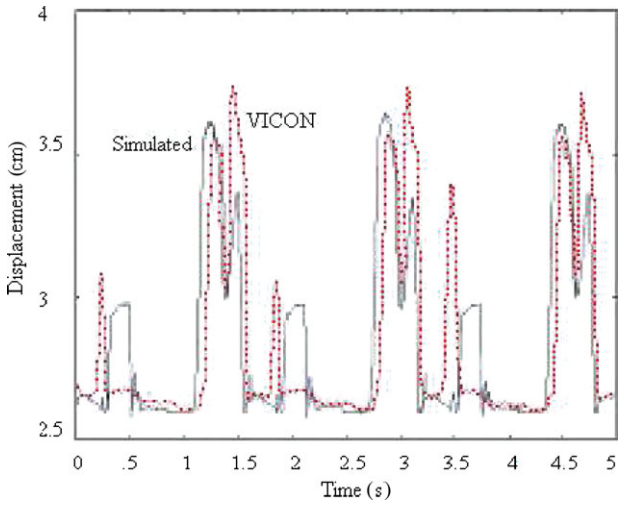

Fig. 11. *Y*-displacement comparison.

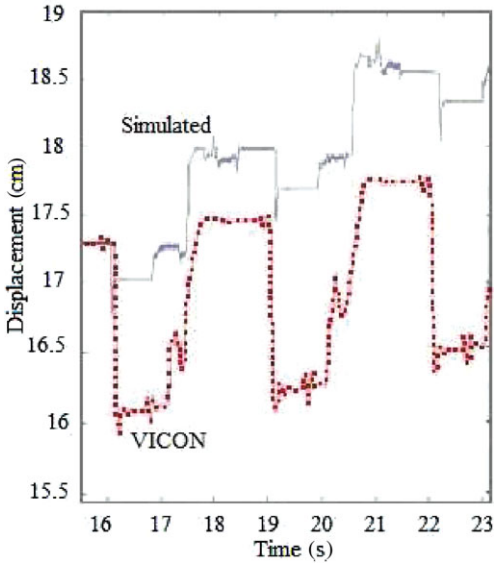

Fig. 12. *X*-displacement comparison.

illustrated in Fig. 14. No clear trend in performance was observed as a function of gait period for this activation pattern. Moreover, the distance traveled per gait period of the wave gait was somewhat lower than four of the 10 evolved gaits implemented in hardware. Setting the period of the traveling wave gait to maximize performance, the resulting distance traveled per gait period was 0.41 cm, which compares to 0.64 cm for the best-evolved gait.

7. Discussion

The experimental results indicate that there is a close coupling between evolved gait periods and the performance

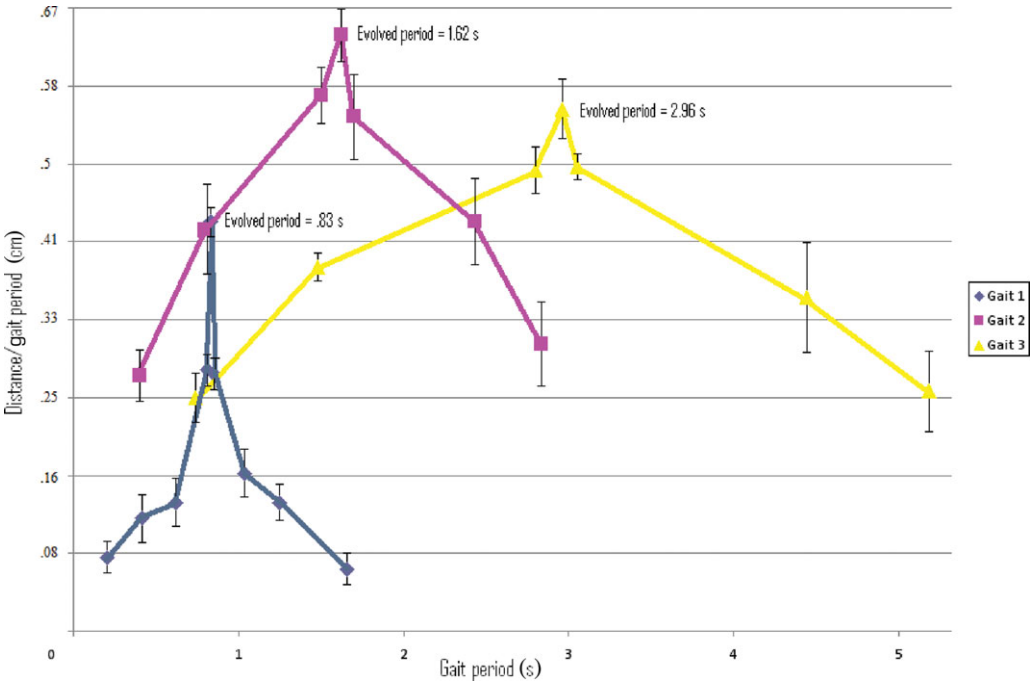

Fig. 13. Gait period effect on distance.

of the soft-robot hardware, as shown in Fig. 13. The fact that robot distance traveled per gait period is maximized at a particular gait duration indicates that the motion is not quasi-static and that dynamics play an important role in gait performance.[26] Moreover, the dramatic decrease in performance away from the evolved gait period, as shown in Fig. 13, provides clear evidence that the simulation captured the system dynamics well enough to enable effective gait optimization. In this sense, the lumped dynamic model appears to be an effective method for modeling certain soft-robot gaits, at least for modeling the caterpillar-like gaits studied in this work. The effectiveness of the lumped element model in simulating the robot dynamics is also supported by the motion capture data, since the motion capture trends closely match the trends predicted by the simulation.

Although the lumped dynamic model resolves essential system dynamics well enough to support gait optimization, the modeling approach did not accurately predict the actual distance traveled by the robot. For these experiments, significant modeling errors were introduced by the pneumatic hoses attached to the robot actuators (see Fig. 1), which create a tension force on the robot, which can be quite large. Qualitative experiments moving the robot toward the hoses (rather than away from the hoses as in the quantitative experiments discussed throughout this paper) suggest that forces from the hoses may account for 30% or more of the discrepancy between the simulation predictions and the experimental results. Additional modeling errors may have resulted from the highly approximate nature of the abstracted robot model, which consisted of only six components (see Fig. 4). Though a more precise physical model might increase the accuracy of the predicted distance simulation, it is, in fact, quite encouraging that this level of accuracy may not be required for the purposes of gait optimization (as illustrated by the experimental data of Fig. 13).

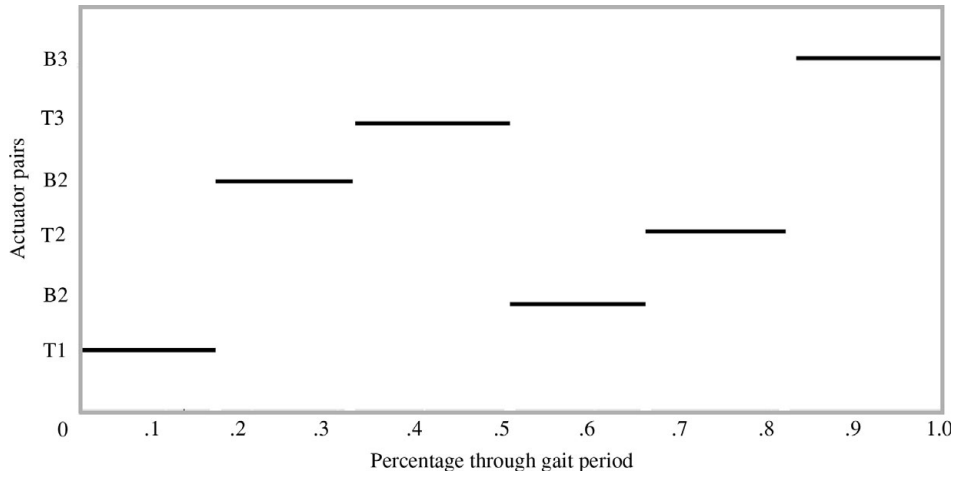

Fig. 14. Intuitive sine wave pattern.

8. Conclusion

This paper investigates whether a lumped dynamic model can be an effective method for designing optimal gait patterns for soft-body robots with distributed actuation. The concept was validated experimentally using a caterpillar-like soft robot. Gait patterns were evolved using a genetic algorithm operating on a lumped dynamic model of the soft robot. Experimental tests showed that the simulations provided only a rough approximation of robot distance traveled per gait period; however, the lumped element model otherwise captured robot dynamics remarkably well. The motion capture data show a close comparison between experimental and simulation results (after accounting for the difference in mean forward displacement per gait period). Most significantly, tests that evaluated gait performance over a range of gait durations demonstrated a dramatic increase in propulsive efficiency precisely at the gait duration optimized by a lumped dynamic simulation. These tests provide strong evidence that the lumped dynamic model captures the essential system dynamics well enough to support gait design and optimization.

Acknowledgments

This work was supported by the DARPA Chemical Robotics Program (DARPA W911SR-08-C-0012). Many thanks to Barry Trimmer for his insights into soft robotics and the locomotion of the caterpillar *Manduca Sexta*.

References

1. A. I. Dobrolyubov, "The mechanism of locomotion of some terrestrial animals by traveling waves of deformation," *J. Theor. Biol.* **119**, 457–466 (1986).
2. J. B. Keller and M. S. Falkovitz, "Crawling of worms," *J. Theor. Biol.* **104**, 417–442 (1983).
3. I. Tanev, "Automated evolutionary design, robustness and adaptation of sidewinding locomotion of a simulated snake-like robot," *IEEE Trans. Robot.* **21**(4), 632–645 (2005).
4. A. J. Ijspeert, "A connectionist central pattern generator for the aquatic and terrestrial gaits of a simulated salamander," *Biol. Cybern.* **84**, 331–348 (2001).
5. L. Chen, S. Ma, Y. Wang, B. Li and D. Duan, "Design and modeling of a snake robot in traveling wave locomotion," *Mech. Mach. Theory* **42**, 1632–1642 (2007).
6. J. Brackenbury, "Fast locomotion in caterpillars," *J. Insect Physiol.* **45**, 525–533 (1999).
7. B. A. Trimmer, A. E. Takesian, B. M. Sweet, C. B. Rogers, D. C. Hake and D. J. Rogers, "Caterpillar Locomotion: A New Model for Soft-Bodied Climbing and Burrowing Robots," *Proceedings of the 7th International Symposium on Technology and the Mine Problem*, Monterey, CA (May 2–5, 2006).
8. W. A. Woods, S. J. Fusillo and B. A. Trimmer, "Dynamic properties of a locomotory muscle of the tobacco hornworm manduca sexta during strain cycling and simulated natural crawling," *J. Exp. Biol.* **211**, 873–882 (2008).
9. R. Pfeifer, M. Lungarella and F. Iida, "Self-organization, embodiment, and biologically inspired robotics," *Science* **318**, 1088–1093 (2007).
10. M. Otake, Y. Kagami, M. Inaba and H. Inoue, "Motion design of a starfish-shaped gel robot made of electro-active polymer gel," *Robotics and Autonomous Systems* **40**, 185–191 (2002).
11. Y. Sugiyama and S. Hirai, "Crawling and jumping by a deformable robot," *Int. J. Robot. Res.* **25**(5–6), 603–620 (2006).
12. M. Otake, M. Inaba and H. Inoue, "Development of a Gel Robot Made of Electro-Active Polymer PAMPS Gel," *Proceedings of the IEEE SMC Conference*, Tokyo, Japan. (Oct. 12–15, 1999), pp. 788–793.
13. J. F. Cuttino, B. Van Dijck and A. M. Brown, "Design and development of a toroidal flexure for extended motion applications," *Precis. Eng.* **29**, 135–145 (2005).
14. K. Autumn, S. Hsieh, D. Dudek, J. Chen, C. Chitaphan and R. Full, "Dynamics of geckos running vertically," *J. Exp. Biol.* **209**, 260–272 (2006).
15. R. Full and D. Koditschek, "Templates and anchors: Neuromechanical hypotheses of legged locomotion on land," *J. Exp. Biol.* **202**, 3325–3332 (1999).
16. S. Kim, J. Clark and M. Cutkosky, "iSprawl: Design and tuning for high-speed autonomous open-loop running," *Int. J. Robot. Res.* **25**, 903–912 (2006).
17. D. Goldman, H. Komsuoglu and D. Koditschek, "March of the sandbots," *IEEE Spectr.* **46**, 30–35 (2009).
18. Y. Moon, "Biomimetic design of finger mechanism with contact-aided compliant mechanism," *Mech. Mach. Theory* **42**(5), 600–661 (2007).
19. P. Dario, C. Stefanini and U. Scarfogliero, "The use of compliant joints and elastic energy storage in bio-inspired legged robots," *Mech. Mach. Theory* **44**(3), 580–590 (2009).
20. Y. Yekutieli, R. Sagiv-Zohar, R. Aharonov, Y. Engel, B. Hochner and T. Flash, "Dynamic model of the octopus arm I: Biomechanics of the octopus reaching movement," *J. Neurophys.* **94**, 1443–1458 (2005).
21. Y. Liang, R. M. McMeeking and A. G. Evans, "A finite element simulation scheme for biological muscular hydrostats," *J. Theor. Biol.* **242**, 142–150 (2006).
22. I. Walker et al., "Continuum Robot Arms Inspired by Cephalopods," **In:** *Unmanned Ground Vehicle Technology VII, Proceedings of SPIE*, vol. **5804** (G. R. Gerhart, C. M. Shoemaker and D. W. Gage, eds.) (SPIE Digital Library, 2005) pp. 303–314.
23. F. Saunders, J. Rieffel and J. Rife, "A Method of Accelerating Convergence for Genetic Algorithms Evolving Morphological and Control Parameters for a Biomimetic Robot," *Proceedings of the IEEE International Conference on Autonomous Robots and Agents (ICARA 2009)*, Wellington, New Zealand (Feb. 10–12, 2009), pp. 155–160.
24. O. Maglino, H. H. Lund and S. Nolfi, "Evolving mobile robots in simulated and real environments," *Artif. Life* **2**, 417–434 (1995).
25. D. Rincon and J. Sotelo, "Dynamic and experimental analysis for inchworm-like biomimetic robots," *IEEE Robots Autom. Mag.* December, 53–57 (2003).
26. J. Rieffel, F. Valero-Cuevas and H. Lipson, "Morphological communication: Exploiting coupled dynamics in a complex mechanical structure to achieve locomotion," *J. R. Soc. Interface* **7**(45), 613–621 (2010).